Design Contours for Complex Marine Systems

Seyffert, Harleigh C.; Kana, Austin A.; Troesch, Armin W.

Important note
To cite this publication, please use the final published version (if applicable).
Please check the document version above.

Design Contours for Complex Marine Systems

H.C. Seyffert[1], A.A. Kana[1] and A.W. Troesch[2]

[1] Delft University of Technology, Delft 2628 CD, The Netherlands,
H.C.Seyffert@tudelft.nl
ORCID id: 0000-0003-0323-2096
[2] The University of Michigan, Ann Arbor MI 48109, USA

Abstract. This paper examines the performance of 6 stiffened ship panel designs in different operational profiles. The main question of interest is: which sea states will lead to the worst panel performances in terms of reliability? As stiffened panel collapse is governed by combined lateral and in-plane loading effects (non-linear functions of the wave environment) this is not a simple problem and does not easily fit into the confines of traditional analyses. Interesting sea states for stiffened panel collapse are identified by a low-order design contour method which uses order statistics and extreme value theory. The resulting multimodal design contours pinpoint areas of interest and the panel performances are confirmed using a higher-order reliability analysis: the non-linear Design Loads Generator process. Such results have impact for creating and interpreting environmental and design contours, as well as assumptions about which operational profiles will lead to the worst system responses.

Keywords: design contours, environmental contours, return period of extreme responses, combined non-Gaussian loading, reliability

1 Introduction

The reliability of marine systems is an important design consideration, but one that is not easily analyzed in the early stages of the design process. Despite continuing advances in computational efficiency, it is generally not feasible to use brute-force simulations in a cell-based approach of each possible operational profile for a long-term probabilistic reliability analysis. Therefore, a common approach is to use a short-term probabilistic analysis in which the presumed "worst-case-scenario" system response is examined due to a few operational profiles, generally known as the equivalent or design sea state method [1].

1.1 Review of Environmental Contour Methods

Sea states which lead to the most extreme loading may be identified by the environmental contour method paired with some coefficient of contribution determination, as in [2]. For marine systems, it is often assumed that a load on a system with a given probability of exceedance is excited by a sea state with that same probability of exceedance. A design sea state is chosen based on the sea

states aligning with the probability contour associated with some allowable risk level along with information about a representative spectral period that maximizes the load variance [3]. Sea states corresponding to rare load responses with very low probabilities of exceedance will have correspondingly short exposures.

The exposure to such harsh excitation is a small fraction of the total expected lifetime, which allows for a short-term probabilistic analysis of the desired load. But in general, failure of marine systems may be due to combined non-linear loading effects. In such cases, the connection between extreme environments, extreme loads, and resulting failure occurrences (or limit surface exceedances) is less clear. To determine the reliability of a system over all possible operational profiles requires information about the ocean excitation, how that environment excites the relevant load effects, and how those load effects interact with some limit surface which determines the occurrence of failure. This paper examines such a system: the collapse of stiffened ship panels due to combined lateral and in-plane loading effects.

Given a set exposure and excitation profile, the reliability of different panel designs can be efficiently examined and compared, as in [4]. For individual linear loads, it is easily determined which excitation regime (short exposure to harsh excitation vs. long exposure to mild excitation) leads to larger load values using extreme value theory (see, e.g., [5]). But stiffened panel failure is due to the combined interaction of lateral and in-plane loading effects with a limit surface which is a non-linear function of panel properties.

For such a system, it is reasonable to question whether a short exposure to the harshest expected environment actually leads to the worst-case system response. Similar risk levels may be possible given a longer exposure to a milder sea state, especially if simultaneous moderate values of combined loading can excite failure. To examine whether this may be possible, this paper expands on the example in [4]. In that paper, the performances of six different stiffened panel designs at a specific location on the David Taylor Model Basin (DTMB) vessel 5415 were compared by the non-linear Design Loads Generator (NL-DLG) process [6]. This paper examines the potential of defining design contours for stiffened ship panels. A low-order design contour method utilizing linear surrogate processes and extreme value theory is presented which identifies sea states which lead to interesting panel performances. As opposed to environmental contour methods which de-couple environmental parameters from structural responses, this low-order model examines the structural response in each possible operational profile in a cell-based approach. The resulting design contour identifies areas of interest which are examined more in-depth by the NL-DLG process. The resulting group of chosen design sea states present a surprising group of sea states which lead to extreme panel reliability responses.

2 Problem Definition

2.1 David Taylor Model Basin 5415 Stiffened Panel Designs

The stiffened panels considered in this paper are potential design options for the inner bottom external shell strake of the DTMB 5415, a modern destroyer-like hull with parameters given in Table 1. The 17th *International Ship and Offshore Structures Congress* (committee V.5 Naval Ship Design) used existing naval structural rules from 6 classification societies to design an optimal stiffened panel (in terms of minimal longitudinal structural weight) for the DTMB 5415 [7], as described in Table 2.

Table 1. DTMB 5415 particulars.

Parameter	Value
Length between perpendiculars (Lpp)	142 m
Length on water line (Lwl)	142.18 m
Beam on water line (Bwl)	19.06 m
Draft (T)	6.15 m
Displacement (∇)	8424.4 m^3
Block Coefficient (CB)	0.507
Longitudinal Center of Buoyancy (LCB) (% Lpp fwd+)	-0.683
Panel Location (fwd of midships +)	13.96 m
Web frame spacing	1905 mm
Stiffener & Plate Yield Stress, σ_Y	355 MPa
Steel Young's modulus, E	200 GPa

Table 2. Panel and stiffener designs for the DTMB 5415 from 2009 ISSC report [7].

Panel	1	2	3	4	5	6
Design pressure [kPa]	$p_{\text{stiffener}} = 60.6$ $p_{\text{web}} = 33.6$	103.6	$p_{\text{stiffener}} = 59.75$ $p_{\text{web}} = 33.89$	86.6	127.45	174.55
Plate thickness [mm]	9	11	8.1	7	8	10
$H_{\text{web}} \times T_{\text{web}}$ [mm]	160×6.2	150×9	154.4×6	113.64×6.35	246.9×5.8	220×6
$H_{\text{flange}} \times T_{\text{flange}}$ [mm]	120×9.8	90×14	101.8×8.9	63×13.36	101.6×6.9	200×6
Stiffener spacing [mm]	672	700	500	364	600	400
Bottom cross-section modulus [m^3]	3.77	4.60	4.14	3.64	3.34	4.93
Weight of longitudinal structure [kg]	16,520	21,121	19,276	15,844	18,329	19,733

2.2 Operational Profile

The reliabilities of these panels are examined for a 30-year lifetime with a prob-ability of non-exceedance $PNE = 0.990$, resulting in a total 300-year exposure. As directed by many classification societies the possible operational profiles are based on the North Atlantic environment described in [8]. The possible signifi-cant wave height-zero crossing period $(H_s - T_z)$ pairs that define the 2-parameter ITTC spectrum for the operational profile are shown in Figure 1, along with the probability of experiencing those sea states over the 300-year exposure. These probability occurrences are defined by [8]. For the sake of brevity in this analysis and to follow [4], only the head seas condition is considered.
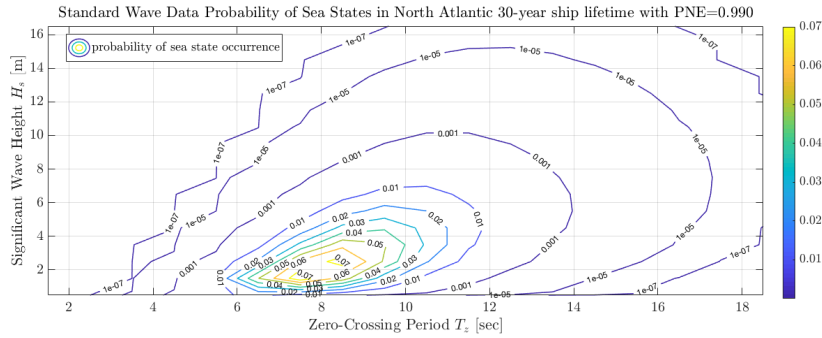
Fig. 1. Probability of occurrence for different sea states in the North Atlantic [8].

3 Methodology

3.1 Stiffened Panel Failure Mechanism & Reliability Estimation

Stiffened ship panels fail due to combined lateral and in-plane loading effects with a limit surface described in the form of Figure 2. A detailed description of the process to define a panel limit surface is given in [9]. In [4], the reliability of the panels described in Table 2 for a 1000-hour exposure in head-seas Hur-ricane Camille-type conditions for failure modes 2-3 was determined using the NL-DLG process [6]. Lateral loading due to slam events (based on the relative velocity between the panel location and the water surface) and in-plane loading effects due to global ship bending are considered as the main loading drivers, restricting the limit surface to just modes 2 and 3, or the first quadrant of Figure 2. The NL-DLG process uses the Design Loads Generator [10, 11] to construct an ensemble of irregular wave profiles which lead to a distribution of extreme responses of a specified linear function corresponding to the given operational profile and exposure period. In the NL-DLG process, linear surrogate processes act as indicators of extreme behavior for the associated non-linear load effects

and estimate which DLG wave profiles excite extreme responses of a system governed by combined non-Gaussian loading.
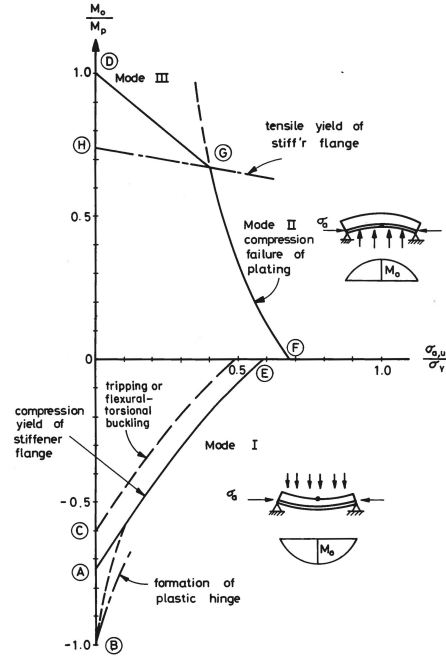

Fig. 2. Limit surface of a stiffened panel due to lateral and in-plane loading effects [9].

3.2 Surrogate Processes of Extreme Loading Effects

As described in [4], extreme relative velocity (RV) at the panel location is an indicator for extreme lateral loading effects on the panel. In the same way, extreme global bending moment (BM) at the panel location is an indicator for extreme in-plane loading effects on the panel. The estimation of the failure probability for the panels in [4] was quite accurate and efficient compared to Monte Carlo Simulations (MCS), indicating that the choice of these surrogates is a good one for the non-linear loading models used. Using linear surrogate processes maintains a clear connection between wave excitation (sea spectrum defined by $H_s - T_z$), extreme vessel "load" responses (RV and BM at the panel location), and characteristics which impact panel reliability (interaction of lateral and in-plane loading effects with the limit surface definition). As another dimension, a criterion is added for a change in vessel speed as a function of the service speed, $V_s = 20$ knots, given the significant wave height. This change in speed based on sea state is often prescribed when assessing lifetime design loads, see, e.g. [12].

$$H_s \geq 10.5 \text{ m } \rightarrow 25\% \text{ of } V_s = 5 \text{ knots}$$
$$10.5 \text{ m} > H_s \geq 7.5 \text{ m } \rightarrow 50\% \text{ of } V_s = 10 \text{ knots}$$
$$7.5 \text{ m} > H_s \geq 4.5 \text{ m } \rightarrow 75\% \text{ of } V_s = 15 \text{ knots}$$
$$H_s < 4.5 \text{ m } \rightarrow 100\% \ V_s = 20 \text{ knots}$$

3.3   Most-Likely Extreme Responses of Surrogate Processes

Using the probability of sea state occurrences from Figure 1 and extreme value theory, contours of the most-likely extreme RV and BM value at the panel location, given the sea state and associated exposure, are constructed and shown in Figures 3-4. The left insets of Figures 3-4 give the most-likely extreme RV and BM value normalized by the respective standard deviation given the sea state and exposure. The right insets give the most-likely extreme RV and BM value for each sea state in physical dimensions (m/s and Nm, respectively).
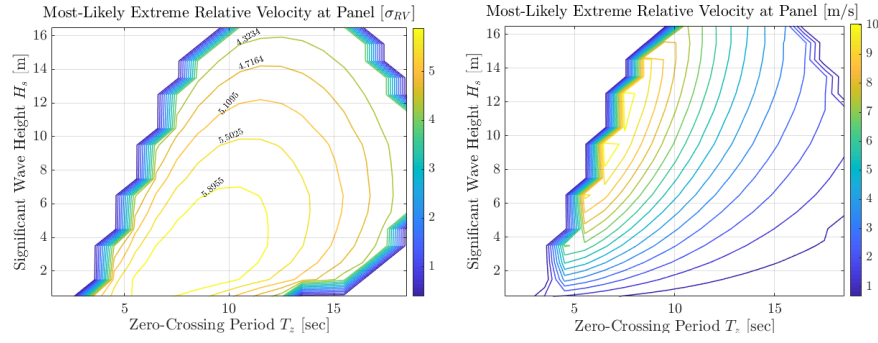
Fig. 3. Left inset: Most-likely extreme RV value (normalized by σ_{RV} associated with the given sea state) at panel location, right inset: most-likely extreme RV value in m/s in the given sea state.

The left insets of Figures 3-4, which give the most-likely extreme RV and BM value as a function of the respective standard deviation describe how rare this extreme value is in the sea state (e.g. a 5σ event) based on the exposure. As the cycle period of RV is much lower than BM there are more RV cycles than BM cycles over a given exposure, meaning the relative extrema of RV are larger than the relative extrema of BM given an operational profile. This is reflected in the left insets of Figures 3-4, in which all of the contours of most likely extreme RV values are at higher σ events than the most-likely BM values at the same sea state. The contours in the left insets indicate how rare an event is, but this does not necessarily mean the magnitude of the most-likely extreme RV or BM value in that sea state will be high, since the process σ value in that particular sea state may be relatively low.
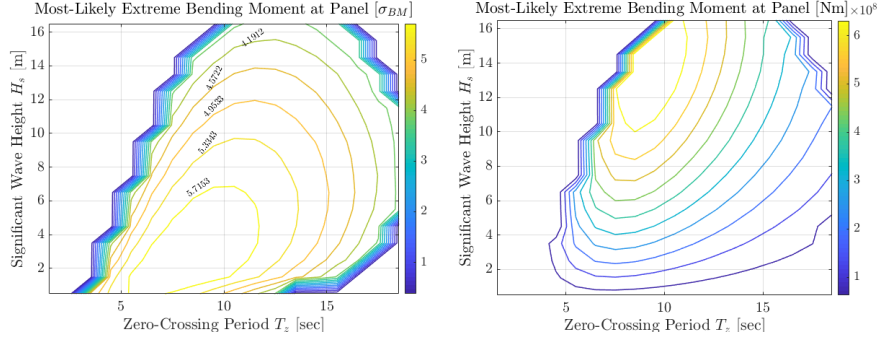
Fig. 4. Left inset: Most-likely extreme BM value (normalized by σ_{BM} associated with the given sea state) at panel location, right inset: most-likely extreme BM value in Nm in the given sea state.

The right insets of Figures 3-4 show that there are specific ranges of wave T_z that lead to large extreme RV and BM values in physical dimensions. However, the range of sea states that lead to the largest most-likely extreme BM values (the brightest yellow contour, right inset of Figure 4) includes many more sea states than the equivalent contour for RV. Note also that the contour of most-likely extreme RV values (in physical dimensions, right inset of Figure 3) is multimodal. This may be due to the fact that the most-likely extreme value is a function of both the process variance and the exposure. The transfer function for the panel RV has a sizable high-frequency content, meaning that sea states with low zero-crossing periods will excite larger RV values.

The exposure associated with a given sea state will also affect the most-likely extreme value, though this most-likely extreme scales with the number of process cycles over the exposure, m, as $\sqrt{ln(m)}$. The variance of RV and BM scales with the variance of the exciting sea state and has a more appreciable impact on the dimensional most-likely extreme value than does the effect of the exposure. However, there are some cases where a lower process variance paired with a long exposure may still lead to an appreciable most-likely extreme RV or BM value. Such a sea state could also lead to poor panel performance.

3.4   Constructing Design Contours using Surrogate Processes

For stiffened panel collapse due to combined lateral and in-plane loading effects, an approximate design contour can be constructed using the surrogate models identified in [4]. In [4], extreme RV and BM at the panel location were identified as good indicators of extreme lateral and in-plane loading effects on the panel, respectively. Therefore, some model reductions can be made to assemble approximate design contours. In this case, the aim of the design contours is not to give an exact estimation of the stiffened panel failure probability given the sea state but to efficiently compare the stiffened panel performance over all possible

sea states to identify sea states of interest. These sea states may then be evaluated by the NL-DLG process, which gives an efficient estimation of the failure probability as compared to brute-force MCS.

Stiffened panel collapse is governed by the panel limit state, which follows the form in Figure 2 and is a non-linear function of the lateral and in-plane loading effects on the panel. The lateral load effect is a non-linear function of the RV at the panel location, and the in-plane loading effect a non-linear function of the global BM at the panel. Even though the lateral and in-plane loading effects are non-linear functions of the RV and BM, respectively, these functions are still one-to-one, meaning the limit surface can equivalently be written as a function of the RV and BM at the panel location. The limit surface described in the BM−RV space is a piece-wise non-linear limit surface as a function of linear effects (BM and RV). The limit surface for each panel in a sea state can further be expressed by the relative weighting of RV and BM by normalizing both axes by the respective standard deviation in the given sea state. Therefore, the limit surface for a panel in the normalized BM−RV space describes the rareness of a BM or RV event required in the given sea state to lead to failure.

A surrogate process can be formulated which is a weighted sum of RV and BM normalized by their respective standard deviations, as in [4], which is described by Equation 1. Each point on the limit surface in the normalized BM−RV space in a given sea state can then be expressed as an individual surrogate process, SP_i, as illustrated in Figure 5 for panel 4.

$$SP_i = \alpha_i \frac{RV}{\sigma_{RV}} + \beta_i \frac{BM}{\sigma_{BM}}$$
$$\alpha_i = \frac{RV_i}{max(RV_g)} \text{ for } g = i, \cdots, n \tag{1}$$
$$\beta_i = \frac{BM_i}{max(BM_g)} \text{ for } g = i, \cdots, n$$

where

$$SP_i = \text{surrogate process } i$$
$$(BM_i, RV_i) = \text{discrete point on the limit surface for a panel in a given sea state}$$
$$max(BM_g) = \text{maximum BM value on the limit surface}$$
$$max(RV_g) = \text{maximum RV value on the limit surface}$$

Visualizing the limit surface for panel 4 in the normalized BM−RV space for the sea state $H_s = 9.5$m $T_z = 6.5$sec already gives a hint about how panel 4 will perform in this sea state. For panel 4 to fail due to extreme lateral loading effects, or extreme RV, (failures on the limit surface near the y-axis), the relative velocity acting at the panel location must be at least a $2.8\sigma_{RV}$ event. Consider that the most-likely extreme RV value in this sea state is $4.2\sigma_{RV}$ (see Figure 3, left inset), and that there is a 63.2% chance that the extreme RV value will be larger than $4.2\sigma_{RV}$. It is expected that panel 4 will often fail when excited by an exposure-period-RV-maximum value in the $H_s = 9.5$m $T_z = 6.5$sec sea state.
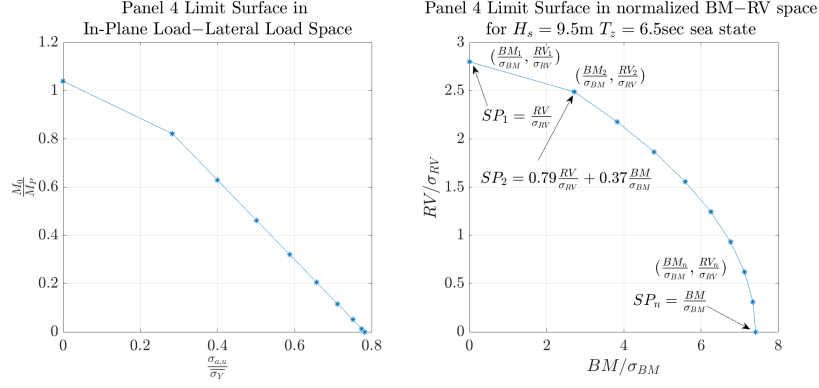
Fig. 5. Limit surface for panel 4 described in the in-plane load−lateral load space (left) and in the normalized BM−RV space given a $H_s = 9.5$m $T_z = 6.5$sec sea state (right).

In the same way, for panel 4 to fail due to extreme in-plane loading effects, or extreme BM, (failures on the limit surface near the x-axis) in the $H_s = 9.5$m $T_z = 6.5$sec sea state, the BM must achieve at least a $7.4\sigma_{BM}$ event. According to the left inset of Figure 4, the most-likely extreme BM value in the $H_s = 9.5$m $T_z = 6.5$sec sea state is $3.98\sigma_{BM}$. It is quite unlikely that this sea state will produce so large a BM event to cause failures in this part of the limit surface. Based on the information about the most-likely extreme RV and BM values in the $H_s = 9.5$m $T_z = 6.5$sec sea state, along with the limit surface in the normalized BM−RV space in this sea state, it is expected that panel 4 will have a high failure probability in the $H_s = 9.5$m $T_z = 6.5$sec sea state, and that any failures will likely be clustered on the limit surface intersect near the y-axis.

As in Figure 5, individual points on the limit surface for each panel in a given sea state can be written as surrogate processes in the form of Equation 1. Since Equation 1 is a linear function of Gaussian inputs (BM and RV) with known transfer functions, it has a known energy spectrum and extreme value distribution. Therefore, for each sea state included in Figure 1, it is easy to calculate the extreme value distribution for each surrogate process SP_i which corresponds to a specific point on the limit surface for a given panel in the normalized BM−RV space for that specific sea state. A low-order estimation for the failure probability in that sea state given waves which excite exposure-period maxima of SP_i is the probability that the most-likely extreme value of SP_i over the exposure exceeds the limit surface value at the location i on the limit surface in the normalized BM−RV space. That is:

$$p(\text{failure for panel } j|SP_i) = p(\text{fail}_j|SP_i) = p(SP_{i,m} > \widehat{sp_{i,m}})$$
$$= 1 - \int_0^{\widehat{sp_{i,m}}} g(sp_{i,m}) \tag{2}$$

where

$g(sp_m)$ = extreme value distribution of surrogate process SP_i, given m process

   cycles over the exposure in the given sea state

$\widehat{sp_{i,m}} = \dfrac{SP_i}{\sigma_{SP_i}} = \dfrac{\alpha_i \frac{RV_i}{\sigma_{RV}} + \beta_i \frac{BM_i}{\sigma_{BM}}}{\sigma_{SP_i}}$ at point i on the limit surface in the normalized

   BM−RV space describing panel j in the given sea state

   In [6], there is a discussion on how to relate failure probabilities conditioned on the system being excited by waves which lead to exposure-period-maxima of a given surrogate process, such as $p(\text{fail}_j|SP_i)$ in Equation 2, to an overall failure probability estimate for panel j. This formulation requires determining how the different surrogate processes SP_i may be related, and the probabilities $p(\text{fail}_j|SP_i)$ are estimated via directed DLG simulations, as opposed to Equation 2. But this overall failure probability estimate for panel j must be at least $p(\text{fail}_j|SP_i)$, given each possible surrogate SP_i. A low-order estimate of the failure probability for panel j in a given sea state is then:

$$p(\text{fail}_j) = \text{maximum}(p(\text{fail}_j|SP_1), p(\text{fail}_j|SP_2), \cdots, p(\text{fail}_j|SP_n)) \qquad (3)$$

4   Results

Using the process described in Section 3, a low-order estimate of the panel failure probabilities given the range of possible operational profiles from Figure 1 can be assembled. Contours of failure probability for each panel design given the operational profile for each sea state are shown in Figure 6. The failure probabilities estimated from Equations 2-3 are a lower bound on the probabilities estimated from the NL-DLG process and what would be expected from brute-force MCS.

4.1   Choice of Sea State given Design Contours

The design contours in Figure 6 bring up some interesting observations about the different panel designs from Table 2. First, clearly these panels do not all have the same general performance characteristics. Panels 3 and 4 both have large ranges of H_s and T_z where a high failure probability is expected. In contrast, the failure probability for panels 5 and 6 across all possible sea states seems to be bounded at about 40%. In addition, the design contours for panels 1, 2, 3, 5, and 6 all exhibit multimodal behavior. Figure 6 also highlights some sea states which are expected lead to interesting panel performances; these are noted as the different markers. The chosen sea states are:

 − $H_s = 9.5\text{m} - T_z = 6.5\text{sec}$: This sea state appears to lead to the maximum failure probability possible for all panels. This sea state also happens to be one of the multimodal maxima for panels 1-3 and 5-6 (panel 4 does not exhibit any multimodal behavior based on Figure 6).
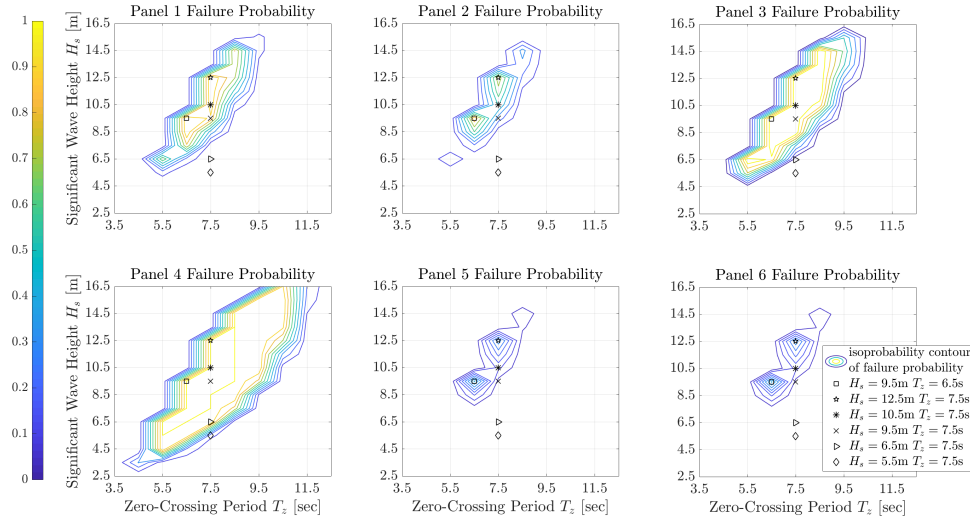
Fig. 6. Contours of failure probability for stiffened panels 1-6 given sea state and exposure. Some potential sea states of interest are highlighted with the different markers.

- $H_s = 12.5$m $- T_z = 7.5$sec: This sea state appears to lead to another instance of maximum failure probability for all panels and represents a different mode for panels 1-2 and 5-6. For panels 3 and 4, this sea state is in the same probability contour as for the $H_s = 9.5$m $- T_z = 6.5$sec sea state.
- $H_s = 10.5$m $- T_z = 7.5$sec: This sea state represents the saddle point between the two peaks in the failure probability contour for panels 2, 5, and 6. For panel 1, this sea state is within the same failure probability contour as for the $H_s = 12.5$m. $- T_z = 7.5$sec sea state.
- $H_s = 9.5$m $- T_z = 7.5$sec: This sea state represents the saddle point between the two major peaks in the failure probability contour for panel 1.
- $H_s = 6.5$m $- T_z = 7.5$sec & $H_s = 5.5$m $- T_z = 7.5$sec: These sea states represent operational profiles which are expected to lead to an appreciable failure probability for a single panel (panel 4) but for no other panel.

The panel failure probabilities based on the contours in Figure 6, estimated using Equation 2-3, along with the sea state and exposure, are given in Table 3. Figure 6 identified a few sea states that may lead to interesting panel responses, with a low-order estimate of the failure probability for that sea state given in Table 3. This reduction of the entire operating space to just a few cases allows a more in-depth analysis of the reliability of the stiffened panels, versus the low-order failure probability estimation offered by Equations 2-3. However, some of the identified sea states have exposure lengths which may be too long for brute-force simulation to be a feasible option. As in [4], the NL-DLG process is used to estimate these failure probabilities, which are given in Table 5.

Table 3. Failure probabilities from low-order design contours in Figure 6.

sea state			contour failure probability for panel j					
H_s [m]	T_z [sec]	exposure [hours]	1	2	3	4	5	6
9.5	6.5	5.26	0.99	0.88	1.0	1.0	0.41	0.41
12.5	7.5	2.63	0.99	0.77	1.0	1.0	0.33	0.33
10.5	7.5	31.55	0.98	0.51	1.0	1.0	0.11	0.11
9.5	7.5	113.03	0.88	0.25	1.0	1.0	0.031	0.032
6.5	7.5	4390	0.0002	0.0001	0.011	1.0	0.0001	0.0001
5.5	7.5	13,101	0.0004	0.0004	0.0004	0.13	0.0004	0.0004

Table 4. Failure probabilities from the NL-DLG process.

sea state			failure probability for panel j					
H_s [m]	T_z [sec]	exposure [hours]	1	2	3	4	5	6
9.5	6.5	5.26	1.0	0.99	1.0	1.0	0.57	0.57
12.5	7.5	2.63	0.99	0.95	1.0	1.0	0.43	0.42
10.5	7.5	31.55	0.99	0.85	1.0	1.0	0.17	0.17
9.5	7.5	113.03	0.95	0.64	1.0	1.0	0.058	0.063
6.5	7.5	4390	0.002	0.0005	0.018	1.0	0	0
5.5	7.5	13,101	0	0	0	0.35	0	0

As expected, the failure probabilities from the low-order estimate of Equations 2-3, presented in Table 3, are a low bound on the failure probabilities estimated by the NL-DLG process in Table 5. Additionally, the sea states identified in Figure 6 for the specific characteristics (maximum failure probability in sea states from disjoint probability contours, saddle point between those disjoint contours, and a sea state which leads to poor performance for a single panel) do produce the expected behavior. The point of the design contours presented in Figure 6 is not to give an exact estimate on the failure probability of the different panels but to give a global comparison between the different panel performances and highlight areas of specific interest for further investigation. The panel performances in these specific sea states are discussed below.

4.2   Sea States leading to Worst Panel Responses

Figure 6 indicated sea states which lead to the worst responses for all panels in terms of reliability, corresponding to the two major disjoint peaks in the probability contours for panels 1, 2, 5, and 6: $H_s = 9.5\text{m} - T_z = 6.5\text{sec}$ and $H_s = 12.5\text{m} - T_z = 7.5\text{sec}$. The NL-DLG process confirmed that both sea states lead to the highest failure probabilities for all examined sea states.

4.3   Sea States Corresponding to Design Contour Saddle Points

Figure 6 indicated that some panels have multimodal contours of failure probability. Two sea states were identified as saddle points between the multiple peaks

of failure probability. The sea state H_s=10.5m $- T_z$=7.5sec represents a saddle point for the failure probability contour for panels 2, 5, and 6. Table 5 confirms that the failure probability for these panels is indeed lower at this saddle point sea state than for the two sea states that maximize failure probability for those panels ($H_s = 9.5$m $- T_z = 6.5$sec and $H_s = 12.5$m $- T_z = 7.5$sec). The sea state $H_s = 9.5$m $- T_z = 7.5$sec represents a saddle point for the failure probability contour for panel 1. Again, Table 5 confirms that this is the case.

4.4   Sea States at Design Contour Boundaries

Two sea states were chosen ($H_s = 6.5$m $- T_z = 7.5$sec & $H_s = 5.5$m $- T_z = 7.5$sec) because they are expected to lead to poor performance for a single panel (panel 4) but negligible failure probabilities for the other panels. Table 5 confirms what may be suspected from Figure 6. These two sea states are only interesting when considering the performance of panel 4. Specifically, for the sea state $H_s = 6.5$m $- T_z = 7.5$sec, where the failure probability for panel 4 is 100% while the other panels have negligible failure probabilities, this result raises an interesting question about the nature of environmental contours. Environmental contours de-couple extreme environmental conditions from structural responses, meaning that the contours have a wide application. The fact that design sea states can be chosen solely from environmental characteristics, without including response characteristics, is noted as an advantage of the method, e.g. [1, 13, 14].

However, the different panel failure probabilities excited by these two sea states illustrate that the structural design strongly impacts whether a sea state leads to interesting design performances. That is, a design sea state may not prove equally interesting for all designs. Picking a sea state simply by the environmental characteristics may not reliably indicate which sea states lead to interesting structural performances. Of course, present design contour methods like the inverse First-Order Reliability Method (IFORM) aim to expand environmental contours to include the limit state of structural response [1]. However, IFORM cannot produce multimodal probability contours. Clearly for some marine systems, traditional reliability and environmental contour methods may not suffice to indicate which sea states may lead to the worst system performances.

4.5   Sea State Harshness of Excitation vs. Exposure Length

A key assumption of environmental contour methods is that the probability of exceeding a load value is associated with the probability of exceeding the harshest sea state which could excite that load, based on the process cycle period. This implies that rare load values are excited by rare sea states, meaning that the exposure to these sea states is likely to be short. It might be natural to say, then, that rare sea states lead to the worst possible system performance. Consider, though, the reliability assessment for panel 4 from Table 5. Clearly panel 4 does not perform well in almost all of the examined sea states. But it is interesting that panel 4 has a 100% failure probability over sea states with many different spectral properties, and crucially, exposure lengths. Panel 4 has a 100% chance

of failure in the $H_s = 12.5$m $- T_z = 7.5$sec sea state, with only a 2.63-hour exposure out of the full 300-year lifetime. But panel 4 also has a 100% chance of failure in the sea state $H_s = 6.5$m $- T_z = 7.5$sec, with a 4390-hour exposure.

Clearly a longer exposure to milder loading can be just as damaging to a system as a much shorter exposure to harsh loading. These sea states have the same T_z, H_s different by a factor of 2, and exposures different by a factor of about 1669. Yet they lead to the same reliability estimate for panel 4. From Figure 6 it might be expected that these two sea states lead to a similar reliability estimate for panel 4. But traditional assumptions about which sea states are expected to lead to the worst-case system responses might not identify the $H_s = 6.5$m $- T_z = 7.5$sec sea state as important. That this sea state can also lead to extreme response for the stiffened ship panel 4 implies that only examining design sea states as identified by traditional environmental contour methods may prove unwise. Extreme responses of complex marine systems may be excited by unexpected sea states given the right combination of T_z, H_s, and exposure.

5   Conclusions

This paper examined the identification of design sea states for complex marine problems like the collapse of stiffened ship panels, which is governed by combined lateral and in-plane loading. Environmental contour methods have been developed because cell-based reliability analysis, in which all possible operational profiles and sea states are individually examined for extreme loads and responses, is generally not a feasible option. Therefore, most environmental contour methods work as an up-down approach. That is, exceedance probability contours of environmental conditions, like H_s and T_z, are first constructed, and design sea states are chosen based on these contours. A key point of such methods is that the environmental conditions and resulting structural response are de-coupled.

In this paper, a bottom-up cell-based approach was instead taken. Using linear surrogate processes along with order statistics and extreme value theory, the structural response to each potential operational profile was examined. With a low-order estimate of the stiffened panel failure probabilities given each cell, design contours over all possible operational profiles were constructed. These contours identified potential design sea states, which were then examined using the higher-order NL-DLG process, which was shown in [4, 6] to estimate failure probabilities accurately compared to brute-force MCS.

The low-order bottom-up approach to design contours presented in this paper avoided some key assumptions of traditional contour methods, and showed how these assumptions may indeed be limitations rather than helpful simplifications. The low-order design contour method used in this paper identified disjoint regions of sea states that lead to similar failure probabilities. Evaluating these sea states ($H_s = 9.5$ m $- T_z = 6.5$sec and $H_s = 12.5$m $- T_z = 7.5$sec) along with the saddle points ($H_s = 10.5$m $- T_z = 7.5$sec and $H_s = 9.5$m $- T_z = 7.5$sec) via the NL-DLG process confirmed the results. By performing a low-order reliability es-

timate cell-by-cell, this multimodal reliability behavior was discovered, whereas in top-down approaches, this multimodal behavior might not be identified.

Additionally, unexpected sea states may also be candidates for design sea states. This was clear for panel 4, where the same failure probability was excited by sea states ranging from a 2.63-hour exposure ($H_s = 12.5\text{m} - T_z = 7.5\text{sec}$) to a 4,390-hour exposure ($H_s = 6.5\text{m} - T_z = 7.5\text{sec}$). In general, this low-order design contour approach illustrated that a design sea state for one design may not be a design sea state for other designs. This was clearly the case for the $H_s = 6.5\text{m} - T_z = 7.5\text{sec}$ & $H_s = 5.5\text{m} - T_z = 7.5\text{sec}$ sea states, which resulted in poor performance for panel 4, but negligible failure probabilities for the rest of the panels. In this case, it may not be beneficial to determine design sea states without including some notion of the design limit state.

Overall, such results indicate that complex marine systems may not easily be analyzed by traditional methods. By employing some specific system simplifications via linear surrogate processes that are indicators of extreme non-linear behavior, interesting design quirks were discovered using order statistics and extreme value theory. The low-order cell-based design contour approach is a potential way to examine complex marine systems and identify sea states which may be good candidates to evaluate reliability and performance under different operational conditions. This has major consequences for designing operational profiles for in-depth numerical or physical models. Design contours as presented in this paper could help direct which sea states are most worth investigating.

6   Acknowledgements

References

1. Winterstein, S., Ude, T., Cornell, C., Bjerager, P., and Haver, S., 1993. "Environmental parameters for extreme response: inverse form with omission factors". *Proc. of Intl. Conf. on Structural Safety and Reliability (ICOSSAR93)*, 01.
2. Baarholm, G. S., and Moan, T., 2000. "Estimation of nonlinear long-term extremes of hull girder loads in ships". *Marine Structures,* **13**(6), pp. 495 – 516.
3. Fukasawa, T., Kawabe, H., and Moan, T., 2007. "On Extreme Ship Responses in Severe Short-Term Sea State". *Advancements in Marine Structures*.
4. H. C. Seyffert and A. W. Troesch and M. D. Collette, 2019. "Combined Stochastic Lateral and In-plane Loading of a Stiffened Ship Panel Leading to Collapse". *accepted: Marine Structures*.
5. Ochi, M. K., 1990. *Applied Probability & Stochastic Processes in Engineering & Physical Sciences*. Wiley series in probability and mathematical sciences.
6. Seyffert, H. C., 2018. "Extreme Design Events due to Combined, Non-Gaussian Loading". PhD thesis, The University of Michigan.

7. Ashe, G., Cheng, F., Kaeding, P., Kaneko, H., Dow, R., Broekhuijsen, J., Pegg, N., Fredriksen, A., de Francisco J. F. Leguen, F. V., Hess, P., Gruenitz, L., Jeon, W., Kaneko, H., Silva, S., and Sheinberg, R., 2009. "17th International Ship and Offshore Structures Congress, Committee V.5 Naval Ship Design".
8. IACS Rec. No. 34, 2001. "Standard Wave Data".
9. Hughes, O. F., 1988. *Ship Structural Design: A Rationally-Based, Computer-Aided Optimization Approach.* The Society of Naval Architects and Marine Engineers.
10. Alford, L. K., 2008. "Estimating Extreme Responses using a Non-Uniform Phase Distribution". PhD thesis, The University of Michigan.
11. Kim, D.-H., 2012. "Design Loads Generator: Estimation of Extreme Environmental Loadings for Ship and Offshore Applications". PhD thesis, The University of Michigan.
12. Lloyd's Register, January 2018. ShipRight Design and Construction, Sttrructural Design Assessment: Global Design Loads of Container Ships and Other Ships Prone to Whipping and Springing. Tech. rep.
13. Baarholm, G. S., Haver, S., and Økland, O. D., 2010. "Combining contours of significant wave height and peak period with platform response distributions for predicting design response". *Marine Structures,* **23**(2), pp. 147 – 163.
14. Vanem, E., 2017. "A comparison study on the estimation of extreme structural response from different environmental contour methods". *Marine Structures,* **56**, pp. 137–162.